Pressure Induced Superconductivity in Pristine $1T$-$TiSe_2$

A. F. Kusmartseva,[1] B. Sipos,[1] H. Berger,[1] L. Forró,[1] and E. Tutiš[2]

[1]*Ecole Polytechnique Federale de Lausanne, IPMC, CH-1015 Lausanne, Switzerland*

[2]*Institute of Physics, P.O. Box 304, HR-10001, Zagreb, Croatia*

(Received 24 July 2009; published 30 November 2009)

The interplay between superconductivity and the charge-density wave (CDW) state in pure $1T$-$TiSe_2$ is examined through a high-pressure study extending up to pressures of 10 GPa between sub-Kelvin and room temperatures. At a critical pressure of 2 GPa a superconducting phase sets in and persists up to pressures of 4 GPa. The maximum superconducting transition temperature is 1.8 K. These findings complement the recent discovery of superconductivity in copper-intercalated $1T$-$TiSe_2$. The comparisons of the normal state and superconducting properties of the two systems reveal the possibility that the emergent electronic state qualitatively depends on the manner in which the CDW state is destabilized, making this a unique example where two different superconducting domes are obtained by two different methods from the same parent compound.

DOI: 10.1103/PhysRevLett.103.236401 PACS numbers: 71.45.Lr, 73.43.Nq, 74.70.Ad

The nature in which superconductivity and other types of electronic order combine continues to remain an ongoing puzzle. Recent findings of superconductivity in copper-intercalated $1T$-$TiSe_2$ triggered a great deal of activity [1–8] due to the possible connection between the superconductivity and the charge-density wave (CDW) state [9–11], and especially as the latter has been proposed as an example of an exciton condensate [12–14]. The superconductivity in Cu_xTiSe_2 was found to arise as the CDW state melts with doping, in a region confined around a critical doping [1]. The dependence of the superconducting transition temperature on the copper content shows a domelike structure, characteristically found in phase diagrams of cuprate high-temperature superconductors, some heavy fermion compounds and layered organics [15–17]. The superconductivity in those compounds is thought to be tightly related to neighboring antiferromagnetic ordering, with superconductivity appearing around a (purely electronic) quantum critical point (QCP) [16,18]. On the other hand the case of $1T$-$TiSe_2$ signals the possibility of a novel state, where superconductivity emerges around a new type of quantum critical point, unrelated to magnetic degrees of freedom [4,8].

An alternative viewpoint regards the proximity of the CDW state and superconductivity in $1T$-$TiSe_2$ as purely coincidental, and the superconductivity as conventional, phonon-mediated, developing in a single band [3]. The formation of the dome structure in $T_{SC}(x)$ is then explained as a consequence of two dissimilar effects produced by doping: (i) the shift of the chemical potential into conduction band caused by the donated electrons and (ii) enhanced scattering at high Cu concentrations, responsible for the reduction of the superconducting transition temperature [3].

In this Letter we report the superconductivity in pure $1T$-$TiSe_2$, studied around sub-Kelvin temperatures, as a function of pressure up to 10 GPa, with the superconducting dome appearing around the critical pressure related to the CDW meltdown. The doping-induced disorder is not present in our system; therefore, impurity effects may not be held responsible for the closing of the superconducting dome.

The single crystal $1T$-$TiSe_2$ samples used in this study were grown by a conventional vapour transport method and the sample stoichiometry was verified by x-ray and resistivity measurements. The resistivity was measured using a standard 4-point technique, with ac lock-in detection. Pressure measurements in the low-pressure range of 0–2 GPa were carried out using a standard piston cylinder pressure cell, while those in the pressure range of 2–10 GPa were performed in an opposed anvil Bridgeman-type pressure cell with tungsten carbide anvils and steatite medium. A dilution refrigeration cryostat was used to achieve base temperatures of 70 mK. Magnetic field for H_c measurements was generated by a superconducting solenoid.

Figure 1 shows the evolution of the resistivity with temperature and pressure. In the low-pressure range up to 1.1 GPa the resistivity curves resemble closely in shape to the one at the ambient pressure [12], although the strong upturn in resistivity that signals the CDW transition becomes gradually less pronounced as pressure increases. Also, the CDW transition temperature, T_{CDW}, identified from the maximum of $-d\rho(T)/dT$ [12], gradually shifts to lower temperature. In this pressure range the resistivity above the transition shows a weak nonmetallic temperature dependence. At temperatures well below the transition the electrons uncondensed into the CDW give the metallic character to the resistivity. Further application of pressure gives rise to the metallic high-temperature region where the resistivity behaves linearly with temperature. Simultaneously the temperature of CDW transition lowers

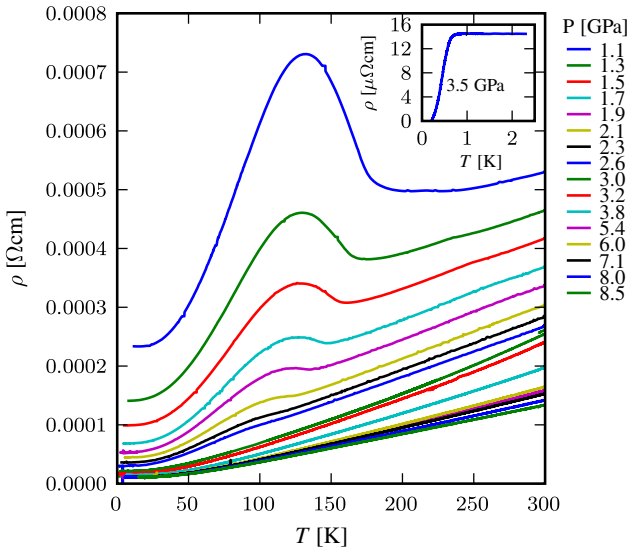

FIG. 1 (color online). Pressure dependent resistivity measurements of $1T$-$TiSe_2$. The ambient pressure run was omitted to emphasize the high-pressure data. For low-pressure data see [19]. The inset shows the emergent superconducting transition at pressures above 3 GPa.

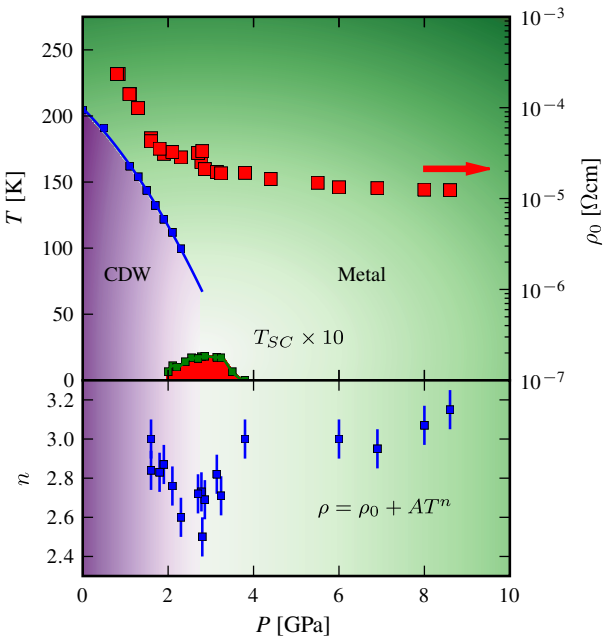

FIG. 2 (color online). Pressure-temperature phase diagram of $1T$-$TiSe_2$. On the left axis we see the evolution of the CDW transition temperature and the superconductivity transition temperature (×10) with pressure. The superconducting dome is constrained to the pressure ranges of 2–4 GPa. On the right axis we see the strong pressure dependence of the residual resistivity over the entire investigated pressure range (note the logarithmic scale). The lower part of the diagram shows the pressure dependence of the thermal exponent n of the resistivity.

monotonically and becomes difficult to identify above 2.5 GPa, disappearing completely above 3 GPa from our resistivity measurements. In the pressure range of 2–4 GPa we observe superconductivity at low temperature (Fig. 1, inset).

Figure 2 summarizes our findings in a pressure-temperature phase diagram. Superconductivity dome appears in the pressure range of 2 GPa around the critical pressure of 3 GPa, where the superconducting transition maximizes with $T_{\mathrm{SC}}^{\mathrm{Max}} \approx 1.8$ K. The residual resistivity, or the resistivity in the normal state just above the superconducting transition at 2 K, shows dramatic variation with pressure until about 4 GPa with only some marginal decrease thereafter, at which point, incidentally, there remains no sign of the superconductivity. Additionally, at the pressure of about 3 GPa there is a local maximum in the residual resistivity, coinciding with the maximum transition temperature of the superconducting dome. On closer examination, we discover a depression in the resistivity temperature exponent n, derived from the standard resistivity fit, $R(T) \approx R_0 + AT^n$, at the same pressure. The resistivity exponent n was obtained through a fitting procedure over the low temperature region of up to 30 K in the data. Outside the superconducting pressure range of 2–4 GPa, the resistivity exponent hovers around the value of $n \sim 3.0 \pm 0.1$. This exponent is different from the expected value of $n = 2$ or $n = 5$ for electron-electron or electron-phonon scattering, respectively, a fact in itself rather unusual. In rare cases where similar behavior is observed, e.g., in Nb_3Ge, Ref. [20], it is commonly attributed to a phonon-assisted s-d interband scattering. A notion proposed by Wilson [21] explains how scattering from a low-mass band into a high-density band can produce higher power law temperature dependence in resistivity. Regardless of the origin of $n = 3$ in $1T$-$TiSe_2$, we observe a sizeable suppression of this exponent in the 2–4 GPa pressure region to a value of $n \sim 2.6 \pm 0.1$ (see lower panel of Fig. 2). These features are reminiscent of a quantum critical scenario, signifying the presence of quantum fluctuations around a critical pressure of 3 GPa. This would complement the quantum critical point recently suggested for Cu-intercalated material, Cu_xTiSe_2, near $x = 0.07$ at ambient pressure [8].

Although pure $1T$-$TiSe_2$ at ambient pressure serves as the starting point for both Cu-intercalation and high-pressure studies, there are several key differences that develop as a function of these two parameters. These go beyond the structural ones, where, in contrast to pressure, the intercalation with copper increases the separation between the layers *as well as* the lattice constants within Ti-Se layers [1]. An earlier report of the sensitivity of the CDW state in $1T$-$TiSe_2$ to pressure [22] also hinted that the electronic state attained through the suppression of the CDW by pressure is qualitatively different from the one recently observed in Cu-intercalated material. The Hall coefficient, R_H, is *negative* in Cu-intercalated material [5], with minor variation in temperature above the CDW transition. Conversely, R_H is always *positive* in the normal state of pure and pressurized $1T$-$TiSe_2$ [22]. The value of

R_H in Cu-intercalated materials is consistent with the assumption that $TiSe_2$ layers become doped by electrons through Cu-intercalation, a rough estimation giving us 0.7 electrons per Cu atom from the $1/R_H$ data. On the contrary, the pressure does not change total concentration of electrons per unit cell in $TiSe_2$ layers, but rather enhances the two-band character of the system by increasing the number of electrons and holes in Ti- and Se-derived bands, respectively [22,23]. The positive R_H reflects the fact that the effective mass of holes in the valence band is approximately 1/20 of the effective mass of electrons in the conduction band [24–26]. This large asymmetry is evidently compensated in Cu-intercalated materials, even for Cu concentrations much lower than those required for the superconductivity to set in [5].

The workings of the collapse of the CDW state are also comparatively dissimilar for pressure and doping. Both mechanisms are rooted in the microscopic nature of the CDW state in $1T$-$TiSe_2$, of which two major viewpoints have emerged over the years [27]. The first one regards the CDW state as an excitonic condensate forming due to the proximity of Se $4p$-derived valence bands and Ti $3d$-derived conduction bands and the Coulomb attraction of holes and electrons in those bands [6,12]. The second viewpoint treats the CDW state exclusively within the electron-phonon coupling framework of a band-type Jahn-Teller (JT) instability [29,30]. Both viewpoints received some experimental support recently through the analysis of the ARPES spectra [6,26,31], with some evidence that both mechanisms might be working simultaneously, and even cooperatively [31,32]. Irrespective of the true nature of the CDW state the pressure and doping will affect it differently. The doping is primarily understood through the shift of the chemical potential within the fixed bands. It is expected to collapse the state of excitonic condensate by introducing a misbalance between two types of charge carriers involved in the creation of the exciton. Similarly, the sensitivity of the JT state to doping is due to the shift of the chemical potential away from the part of the electronic spectrum that becomes depleted with lattice deformation. Conversely, the pressure acts by shifting whole valence and conduction bands and increasing their overlap in energy [22,23]. This dislodges the excitonic phase outside the window of stability as proposed by Halperin and Rice [33]. The increase of the overlap of two bands pushes the Fermi level further into both bands, away form the band edges. This also reduces the possibility of the band-JT instability, with a deformation that would significantly reduce the density of states near the Fermi level.

Another important indication which suggests that the situation in pressurized and Cu-intercalated $1T$-$TiSe_2$ may be qualitatively different comes from quantifying the influence of the magnetic field on the superconducting state, presented in Fig. 3 for the pressurized material. The value of the critical field, taken as the 10% drop of the normal state resistivity signal, is approximately 200 Gauss at 3.5 GPa. Therefore, the superconductivity in pure $1T$-$TiSe_2$ is extremely sensitive to magnetic field, in sharp contrast to the critical field values of the order of 1 T obtained for the Cu-intercalated system Cu_xTiSe_2 [1], although detailed doping and pressure dependencies for H_c for both these systems would be needed for a more precise comparison.

In conclusion, the results of the present Letter strongly suggest that the CDW fluctuations are tightly linked with superconductivity in $1T$-$TiSe_2$. The parallels with several families of materials where the superconducting dome has been discovered in the vicinity of purely electronic ordered phase, dressing the quantum critical point [16–18] strengthen the viewpoint of excitonic superconductivity in $1T$-$TiSe_2$. On the other hand, the continuous development of the soft phonon mode in the vicinity of the CDW transition, both in Cu-intercalated and pure and pressurized material [8,34,35], suggests that the lattice deformation may not be regarded as a secondary effect that simply follows the electronic ordering. The soft phonon mode, generally regarded as unfavorable for superconductivity within the weak-coupling BCS single-phonon exchange picture, has been identified as helpful in several instances for higher values of the electron-phonon coupling [36–39]. This marks an alternative route for searching for the origin of the superconducting dome in $1T$-$TiSe_2$.

The new phase diagram of pristine $1T$-$TiSe_2$ under pressure complements and puts in a new light recently reported superconductivity in Cu-intercalated $1T$-$TiSe_2$. Figure 4 summarizes our knowledge of the phase diagram

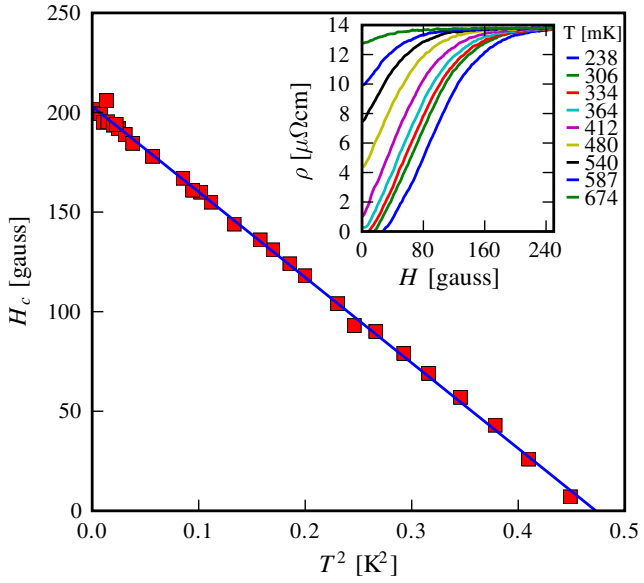

FIG. 3 (color online). Temperature dependence of the magnetic critical field in $1T$-$TiSe_2$ at the pressure of 3.5 GPa, in the temperature range 70–700 mK, shown as a function of T^2. The data follow rather well the full straight line which stands for $H_c(0)(1 - T^2/T_{SC}^2)$ The values for H_c were derived from the 10% drop of the normal state resistivity signal from the resistivity-field isotherms.

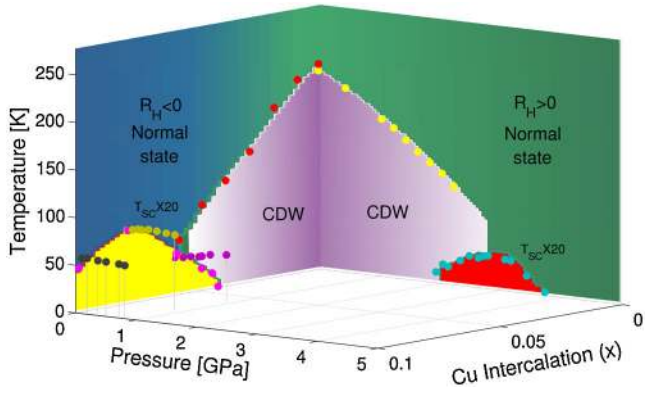

FIG. 4 (color online). The present knowledge of the phase diagram of 1T-Cu_xTiSe_2, where the horizontal axes stand for pressure and the content x of the intercalated copper. The ambient pressure data are from Ref. [1], the points for finite doping and pressure below 1 GPa are from Ref. [2], while the data for the pressurized material without copper are from the present study. The empty space between two superconducting domes on the axes suggests future investigations in this compound.

of 1T-$TiSe_2$ in the temperature, pressure and copper doping content parameter space. The absence of dopands in our case implies that the closure of the superconducting dome is unrelated to impurity-induced scattering. Given the similarities between the intercalated and the pressurized system, analogous reasoning may be extended for Cu-intercalated system. On the other hand we also point out the qualitative differences in electronic states that develop along P and x axis, marked by opposing signs of the Hall coefficient in the normal state, different maximum superconducting transition temperatures T_{SC}^{Max} (1.8 K versus 4.15 K for pressure and intercalation, respectively) and diverse magnetic properties in the superconducting state. These dissimilarities leave open the question whether two separate superconducting domes develop in this phase diagram, corresponding to two distinct critical points. The alternative perspective of a critical line in the $T = 0$ plane of Fig. 4, covered by the ''superconducting tunnel'', is a challenging topic for future studies.

The work was supported by the Swiss National Science Foundation (SNSF) and its NCCR ''MaNEP'', by the Croatian MZES Project No. 035-0352826-2847, and by the SCOPES Project No. IB7320-111044.

[1] E. Morosan *et al.*, Nature Phys. **2**, 544 (2006).
[2] S. L. Bud'ko *et al.*, J. Phys. Condens. Matter **19**, 176230 (2007).
[3] J. F. Zhao *et al.*, Phys. Rev. Lett. **99**, 146401 (2007).
[4] S. Y. Li, G. Wu, X. H. Chen, and L. Taillefer, Phys. Rev. Lett. **99**, 107001 (2007).
[5] G. Wu *et al.*, Phys. Rev. B **76**, 024513 (2007).
[6] H. Cercellier *et al.*, Phys. Rev. Lett. **99**, 146403 (2007).
[7] D. Qian *et al.*, Phys. Rev. Lett. **98**, 117007 (2007).
[8] H. Barath *et al.*, Phys. Rev. Lett. **100**, 106402 (2008).
[9] J. A. Benda, Phys. Rev. B **10**, 1409 (1974).
[10] J. A. Wilson and S. Mahajan, Commun. Phys. **2**, 23 (1977).
[11] J. A. Wilson, A. S. Barker, F. J. DiSalvo, and J. A. Ditzenberger, Phys. Rev. B **18**, 2866 (1978).
[12] F. J. Di Salvo, D. E. Moncton, and J. V. Waszczak, Phys. Rev. B **14**, 4321 (1976).
[13] W. Kohn, Phys. Rev. Lett. **19**, 439 (1967).
[14] R. S. Knox, *Solid State Physics, Supplement* (Academic Press, New York, 1963), Vol. 5, p. 100.
[15] P. A. Lee, N. Nagaosa, and X.-G. Wen, Rev. Mod. Phys. **78**, 17 (2006).
[16] V. A. Sidorov *et al.*, Phys. Rev. Lett. **89**, 157004 (2002).
[17] J. Wosnitza, J. Low Temp. Phys. **146**, 641 (2007).
[18] J. L. Tallon *et al.*, Phys. Status Solidi B **215**, 531 (1999).
[19] See EPAPS Document No. E-PRLTAO-103-035950 for supplementary material. For more information on EPAPS, see http://www.aip.org/pubservs/epaps.html.
[20] D. W. Woodard and G. D. Cody, Phys. Rev. **136**, A166 (1964).
[21] A. H. Wilson, Proc. R. Soc. A **167**, 580 (1938).
[22] P. C. Klipstein and R. H. Friend, J. Phys. C **17**, 2713 (1984).
[23] R. H. Friend and A. D. Yoffe, Adv. Phys. **36**, 1 (1987).
[24] N. G. Stoffel, S. D. Kevan, and N. V. Smith, Phys. Rev. B **31**, 8049 (1985).
[25] T. Pillo *et al.*, Phys. Rev. B **62**, 4277 (2000).
[26] K. Rossnagel, L. Kipp, and M. Skibowski, Phys. Rev. B **65**, 235101 (2002).
[27] Antiferroelectric instability has been also proposed [28].
[28] A. Bussmann-Holder and A. R. Bishop, Phys. Rev. B **79**, 024302 (2009).
[29] H. P. Hughes and W. Y. Liang, J. Phys. C **10**, 1079 (1977).
[30] N. Suzuki, A. Yamamoto, and K. Motizuki, J. Phys. Soc. Jpn. **54**, 4668 (1985).
[31] T. E. Kidd, T. Miller, M. Y. Chou, and T.-C. Chiang, Phys. Rev. Lett. **88**, 226402 (2002).
[32] J. van Wezel, P. Nahai-Williamson, and S. S. Saxena, arXiv:0907.1836v1.
[33] B. I. Halperin and T. M. Rice, Rev. Mod. Phys. **40**, 755 (1968).
[34] M. Holt, P. Zschack, H. Hong, M. Y. Chou, and T. C. Chiang, Phys. Rev. Lett. **86**, 3799 (2001).
[35] C. S. Snow, J. F. Karpus, S. L. Cooper, T. E. Kidd, T. C. Chiang, Phys. Rev. Lett. **91**, 136402 (2003).
[36] J. Appel, Phys. Rev. **180**, 508 (1969).
[37] A. Bussmann-Holder and A. Bishop, Z. Phys. B **86**, 183 (1992).
[38] M. Nohara *et al.*, Phys. Rev. Lett. **70**, 3447 (1993).
[39] R. Lortz *et al.*, Phys. Rev. B **73**, 024512 (2006).